

SVC adaptive controller based on ANN by using radial basis function and multilayer perceptron to improve voltage stability

KADIR ABACI^{*}, ZAFER ÖZER^a, M. ALI YALÇIN^b, ERCAN KÖSE^c

Electrical and Electronics Engineering Department, Mersin University, Turkey

^a*Departement Distance learning, Tece Campus, Mersin University, Turkey*

^b*Electrical and Electronics Engineering Department, Esentepe Campus, 54187, Turkey*

^c*Mechatronics Engineering Department, Tarsus Campus, Mersin University, Turkey*

Reactive power control is the most efficient and popular voltage control method, especially for variable active power demand. Static Var Compensators (SVCs) are being increasingly employed in modern power systems. This paper proposes an Artificial Neural Network (ANN)-based Static Var Compensator (SVC) controller and a novel bus reducing method for power systems. Two types of artificial neural network controllers namely are Multi-Layer Perceptrons (MLP) with back propagation learning algorithm, and Radial Basis Function (RBF) network are used. In the simulations, a variable power demand is modelled as a disturbance effect and voltage stability control was done at the operating points with SVC. It is shown that the voltage output was successfully regulated and desired voltage value are obtained quickly. Transient responses for voltage and susceptance show that SVC controller with ANNs provide optimum system performance for a disturbance effect. Performance of ANN based SVC controllers were tested. The effectiveness and feasibility of the proposed control is demonstrated with the simple two bus system and three-machine nine-bus WSCC system. The results show that improvement especially ANN based RBF controller has better performance the MLP based controller.

(Received May 20, 2014; accepted March 19, 2015)

Keywords: Voltage Stability, Artificial Neural Network (ANN), Multi-Layer Perceptrons (MLP), Radial Basis Function (RBF), Static Var Compensator (SVC)

1. Introduction

Due to the environmental limitations and immense cost of building new transmission lines, available power systems are operating ever closer to their utility limits with the fast increase of load demand. As a result, many power grids are highly stressed and voltage instability problem poses a primary threat to system stability, security, and reliability.

Voltage collapse and other instability problems are often related to the inability of the system to meet reactive power demands. The power system control technique has been developed with the advancement of power electronic technologies that introduce new degrees of freedom into the operation of power system. It is found that Flexible AC Transmission System (FACTS) devices are good choice to improve the voltage profile and stability in a power system, which operates near the steady-state stability limit and may result in voltage instability.

Lately, with the improvement of power electronic technologies, several FACTS devices make it possible to control power flows and bus voltages. [1-2].

The SVC has been widely used in power system which are well known to improve power system properties such as steady-state stability limits, voltage regulation and VAr compensation, dynamic over-voltage and under voltage control, and damp power system oscillations[3-4]

for both voltage regulation and dynamic stability enhancement.

Nowadays, SVC control is increasingly applied in power systems. Some conventional method have been used in previous research for control of SVC [5-6], Hopf bifurcation control [7], nonlinear and H_{∞} control [4-7-8], adaptive control [9], PID [10] and fuzzy- PID control [11-12], Intelligent controller [13], fuzzy logic[14-15] and neuro-fuzzy controller [16], optimal predictive controller [17], nonlinear and nonlinear robust controller [18-19].

Artificial neural network (ANN) is considered as an important method of artificial intelligence and it is being used successfully in many areas of power systems, such as power system control, of system values prediction etc. [20-21]. Load forecasting, dynamic security assesment, fault diagnosis, etc. are discussed In [22] interesting applications of ANN to power systems.

In voltage stability works the control of reactive power is a practical and useful method in heavily loaded systems. Susceptance value is achieve desired value.

In this paper, a satisfactory controller, incorporated in the system, is developed by using ANN. A suitable susceptance for stable operation can be generated by voltage error. The error of the output and desired voltage has been used to regulate/ produce a constant voltage output.

In this work detailed analysis of two kinds of ANN based controllers, MLP and RBF are given. Results of simulation studies are presented to illustrate the effectiveness of the proposed controller and damped oscillations. It is trained online. At the end of online training, it is enabled to reach the desired value. The main advantage of the proposed controller is easy adaption for critical loading values and fast reply capability. The responses show that the proposed controller has the ability to restore the power system stability in short time with less overshoot. The voltage stability control with SVC values which drag the operating load values of the example of power system into instability is tested successfully.

2. Differential algebraic power system model

In general, power systems are modeled by the following set of differential and algebraic equations

$$\begin{aligned} \dot{x} &= f(x, y, \mu, p) \\ 0 &= g(x, y, \mu, p) \end{aligned} \quad (1)$$

where $x \in \mathfrak{R}^n$ is a vector of state variables associate with dynamic states of generators, loads, and other system controllers; $y \in \mathfrak{R}^m$ is a vector of algebraic variables associate with steady-state variables resulting from neglecting fast dynamics, e.g., some load voltage phasor magnitudes and angles, etc; $\mu \in \mathfrak{R}^k$ is a set of uncontrollable parameters, such as active reactive power load variations; and $p \in \mathfrak{R}^l$ is a set of controllable parameters such as SVC susceptance.

For the eigenvalue analysis (small signal stability or steady state stability analysis), (1) can be linearized around an equilibrium point (x_0, y_0) for given values of the parameters (μ, p) (an operating points). Thus,

$$\begin{bmatrix} \Delta \dot{x} \\ 0 \end{bmatrix} = \underbrace{\begin{bmatrix} J_1 & J_2 \\ J_3 & J_4 \end{bmatrix}}_J \begin{bmatrix} \Delta x \\ \Delta y \end{bmatrix} \quad (2)$$

where, J is a system in Jacobean matrix form, and $J_1 = \partial f / \partial x|_0$, $J_2 = \partial f / \partial y|_0$, $J_3 = \partial g / \partial x|_0$, $J_4 = \partial g / \partial y|_0$. If it is assumed that J_4 is nonsingular, the system eigenvalues can be readily computed by eliminating the vector of algebraic variable Δy in (2), $\Delta \dot{x} = (J_1 - J_2 J_4^{-1} J_3) \Delta x = A \Delta x$ i.e., the DAE system can be reduced to a set of ODE equations [23].

2.1. Saddle Node Bifurcation (SNB)

This equilibrium is typically associated to a saddle node bifurcation. At a SNB point, two equilibrium points,

generally one stable and one unstable, coalesce and become a saddle-node point, and then disappear as the parameter passes through the bifurcation value. For the SNB, J has a simple zero eigenvalue with the remaining eigenvalues having non-zero real parts. Therefore, the necessary conditions for SNB are given by

The first condition:

$$f(x_0, \lambda_0) = 0 \quad (3a)$$

The second condition:

$$\det J((x_0, \lambda_0)) = 0 \quad (3b)$$

where, J is a system Jacobian, SNB is considered as a main reason for dynamic instability of the system (3) and associated with voltage collapse problems in power systems [24-25].

3. Simple power system

The simple two bus system is shown in Fig. 1. The p.u dynamic equation (4)-(5) that represents this system using a generator classical model, a frequency and voltage dependent dynamic model for the load (Eq.6) are given by

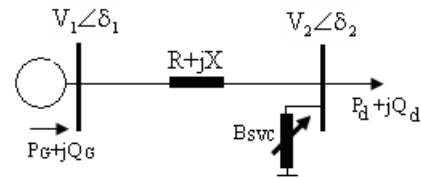


Fig. 1. Basic power system having SVC at the end of transmission line.

Generator swing equations are given by

$$\dot{\delta} = w \quad (4)$$

$$\dot{w} = \frac{1}{M} (P_m - P_G - D_G w) \quad (5)$$

The dynamic equations for load at a bus are given by:

$$\dot{V}_2 = \frac{1}{\tau} (Q_L - Q_D) \quad (6)$$

where the generator inertia and damping constants are represented by M and D_G , τ stands for voltage time constants [26]. In this case, the power flow equations are given as following

$$\delta = \delta_1 - \delta_2, \quad G = \frac{R}{R^2 + X^2}, \quad B = \frac{X}{R^2 + X^2}$$

Algebraic equations for power system in

$$P_G = V_1^2 G - V_1 V_2 (G \cos \delta - B \sin \delta) \quad (7)$$

$$P_L = V_2^2 G + V_1 V_2 (G \cos \delta + B \sin \delta) \quad (8)$$

$$Q_G = V_1^2 B - V_1 V_2 (G \sin \delta - B \cos \delta) \quad (9)$$

$$Q_L = -V_2^2 (B - B_{SVC}) - V_1 V_2 (G \sin \delta - B \cos \delta) \quad (10)$$

Q_G is used to represent generator reactive limits. If $Q_{G_{\min}} \leq Q_G \leq Q_{G_{\max}}$, the generator voltage V_1 is assumed to be controlled to represent somewhat the control actions of a voltage regulator or AVR; thus, neglecting droop and the control system dynamics, the voltage regulator is modeled hereby keeping the generator terminal voltage at the fixed value $V_1 = V_{10} = 1$

3.1 An illustrative example: Single-Machine Dynamic-Load system with SVC

An illustration for SVC is widely used in power systems to control the voltage at the load bus of the SMDL system, as illustrated in Fig. 1.

SVC has been represented by dynamic SVC Model- [27].

$$\dot{B}_C = \frac{1}{T} (V_{ref} - V_2) \quad (11)$$

where B_C is the equivalent susceptance of the SVC, T and V_{ref} are the SVC time constant and reference voltage, respectively. In the following, it is assumed that $T = 0.01$ s and $V_{ref} = 1.0$ p.u. Observe that, also in this case, it is possible to deduce the set of ODE, i.e., the algebraic variables can be explicitly expressed as a function of the state variables and the parameters.

The state matrix of (4-5-6-11) is as follows

$$J = \begin{bmatrix} 0 & 1 & 0 & 0 & 0 \\ 1 & -\frac{D_G}{w} & -\frac{1}{M} V_1 (G \cos \delta - B \sin \delta) & 0 & 0 \\ \frac{1}{\tau} V_1 V_2 (G \cos \delta + B \sin \delta) & 0 & \frac{1}{\tau} (-2V_2 (B - B_C) - V_1 (G \sin \delta - B \cos \delta)) & \frac{V_2^2}{\tau} & 0 \\ 0 & 0 & -\frac{1}{\tau} & 0 & 0 \end{bmatrix}$$

Fig. 2 depicts the P_d - V curve for the simple power system. SNB points are $X_0 = [w_0; \delta_0; V_0; B_{C0}; P_{d0}] = [0.0; 0.6629; 0.6343; 0.0; 0.78078]$, $[0.0; 0.6629; 0.0; 0.6677; 0.1; 0.8218]$ and $[0.0; 0.6629; 0.7048; 0.2; 0.8675]$ for $B_C = 0$, $B_C = 0.1$ pu and B_C

$= 0.2$ pu respectively. The voltage stability margin is therefore increased. The return points in Fig 2. are increased by applying higher B_C values.

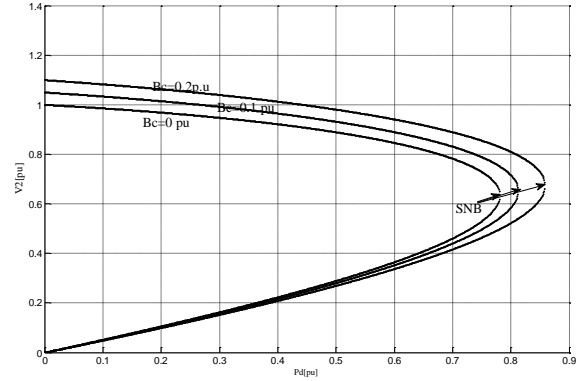


Fig. 2. Bifurcation diagram (P_d - V curve).

4. Neural control

Neural control refers to a methodology in which the controller itself is a neural network, and it is also to a methodology in which controllers are designed based on a neural network model of the plant. These two basically different approaches for implementing neural networks in control are defined as direct and indirect design methods.

Specifically, when mathematical models of the plant dynamics cannot be calculated, neural networks can provide a useful method for designing controllers and numerical information about the system behavior in the form of input-output data.

Basically, to build a neural network based controller that can force a plant to behave in some desirable way, we need to adjust its parameters in terms of the observed errors that are difference between the plant's outputs and desired outputs. Adjustment of the controller parameters can be achieved by propagating back these errors across the neural network structure [28].

There are many different types and architectures of NNs varying fundamentally in the way they learn, the details of which are well documented in literature. In this study, the multi layer perceptron and radial basis function are used as a SVC controller by using Neural Network Toolbox of Matlab/Simulink [29].

4.1 Proposed multi-layer perceptron neural networks

Multi-layer perceptrons cover a large group of feed-forward neural networks with one or more layers of neuron. In most applications, MLP networks have three layers in addition to input and output layers. Neurons in input layer have a pure linear activation function, but some nonlinear activation functions such as logarithmic and hyperbolic tangent functions are used in the neurons in hidden and output layers [30]. The multilayer feed-forward ANN shown in Fig.1. will be used in this work to adapt

the controller of the SVC in real time. Before the ANN is adapted to the controller in real time, it is necessary to determine a proper set of values for the connecting weights v_{ji} and w_{kj} .

The input and output values of the hidden layer are denoted x_i and y_j , respectively. We thus denote x_i , for $i = 1, 2, \dots, I$, and y_j , for $j = 1, 2, \dots, J$, which defines signal values at the i 'th column of nodes, and j 'th column of nodes, respectively. Using the vector notation, the forward pass of the hidden neurons in the network shown in Fig. 2 can be expressed as follows

$$y = \Gamma[Vx] \quad (12)$$

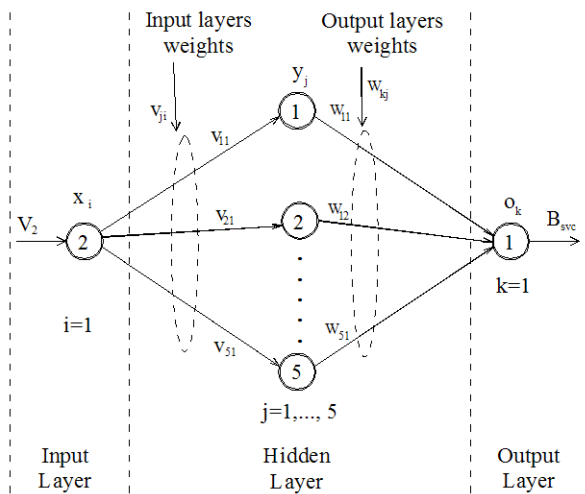


Fig. 3. Multilayer feed-forward ANN.

The input and output values of the output layer are denoted y_j and o_k , respectively. We thus denote y_j , for $j = 1, 2, \dots, J$ and o_k , for $k = 1, 2, \dots, K$, which represents signal values at the j 'th column of nodes, and k 'th column of nodes, respectively. Using the vector notation, output of the network can be expressed as follows

$$o = \Gamma[Wy] \quad (13)$$

which includes input, output vectors, the weight matrix as mentioned and Γ defines nonlinear diagonal operator [31].

Activation function used in hidden layers is a hyperbolic tangent function that can be derived. This function is similar to logistic function between +1 and -1. Its equation is mentioned as below. Linear activation function is used in output layer.

$$f(x) = \tanh(x) = \frac{e^x - e^{-x}}{e^x + e^{-x}} \quad (14)$$

In this study, generalized delta rule is used as a learning rule, and weights are updated according to the errors between network and desired outputs. Hence, this algorithm is called as a back propagation algorithm. Training process of the back propagation algorithm runs according to the following steps [32]

Step 1: Initialize all weights at random

Step 2: Submit pattern x and compute layers' responses

$$y = \Gamma[Vx], \quad o = \Gamma[Wy]$$

Step 3: Compute cycle error

$$E = \frac{1}{2} \sum_{k=1}^K (d_k - o_k)^2$$

Step 4: Calculate errors δ_o, δ_y

$$\delta_o = \frac{1}{2} [(d_k - o_k) (1 - o_k^2)]$$

$$\delta_y = w_j^t \delta_o f_y'$$

Step 5: Adjust weights of output layer

$$W' \leftarrow W + \eta \delta_o y^t$$

Adjust weights of hidden layer

$$V' \leftarrow V + \eta \delta_y x^t$$

Step 6: Iterate the calculation by returning to Step 2 until the error is less than the desired error.

where δ_o and δ_y , are the column vector with entries δ_{ok} are δ_{yj} respectively

4.2 Proposed radial basis function neural networks

RBF networks have been proposed and used as an alternative to the MLP network for many engineering problems. Architecture of a RBF network is similar to a MLP network. RBF networks have three layers called as input, hidden and output layers like MLP networks. The neurons within each layer are fully connected to the previous layer neuron. However, input variables are directly transferred to the hidden layers. The connections between input and hidden layers do not have any weight coefficient. So, neurons in the hidden layer receive the incoming input variables with an unchanged situation [33]. In this study, a typical RBF structure is used as illustrated in Fig. 4.

Radial basis Gaussian Function (15) is considered as transfer function in this study

$$\psi(u, c, \sigma) = e^{-\left(\frac{u-c}{\sigma}\right)^2} \quad (15)$$

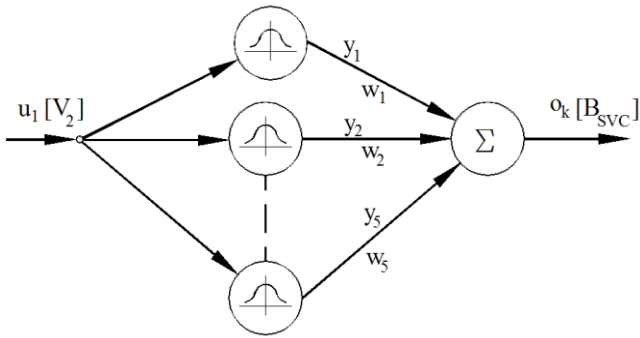


Fig. 4. RBF neural network.

where c is the center, σ is the variance and u is the input variable. The output of the k 'th neuron in the output layer at time

$$y_k = \prod_{j=1}^m \psi(u_j, c_j, \sigma_j) \quad (16)$$

5. layer is the hidden layer as shown in Fig. 3. The output of each neuron is calculated by using Equation 17 and is used in 4.3. with weights. Here, w_i is weight parameter and H is number of hidden layer,

$$o_k = \sum_{i=1}^H w_i y_i = \sum_{i=1}^H (w_i (\prod_{j=1}^m \psi(u_j, c_j, \sigma_j))) \quad (17)$$

Traning process of the radial basis function neural network runs according to the following steps [34]

Step 1: Initialize all weights at random

Step 2: Submit pattern u and compute layers' responses. Use

$$Y_k = \prod_{j=1}^m \psi(u_j, c_{ij}, \sigma_{ij}), o = \Gamma[WY]$$

Step 3: Compute cycle error

$$E = \frac{1}{2} \sum_{k=1}^K (d_k - o_k)^2$$

Step 4: Adjust weights of output layer

$$W' \leftarrow W + \eta \frac{\partial E}{\partial w}$$

Step 5: Iterate the calculation by returning to Step 2 until the error is less than the desired error.

4.3 Application of ANN to adapt SVC controller

The proposed training structure is shown in Fig. 5. In the proposed methods, we used an adaptive controller. The controller is referred as “adaptive” due to the continuity of the learning process. The objective is to train the neural network in such a way that the controller will enable the plant to produce the desired outcome. To achieve this, the

neural network should be trained in such a way that the input of error $e(t)$ produces the proper control parameter $u(t)$ which will be applied to the plant to produce $y(t)$ [30].

The multilayer feed forward and RBFNN controller have one input and one output as illustrated in Fig. 3 and Fig. 4.

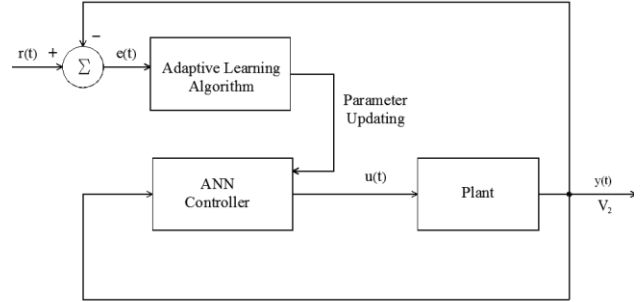


Fig. 5. Proposed neural network controller.

The neural network controller is trained online, and produces an appropriate SVC susceptance in order to catch the reference signal. There are five neurons in the hidden layer. The hidden layer has nonlinear activation functions, and the output layer has a linear activation function. For every input, the function produces an output. The parameters of ANN are updated by using the error between the ANN output and the reference model. Network architecture is given in Table 1. Gaussian function in hidden layer and linear activation function of output layer is used.

Table 1. Structure of trained Neuro-Controllers.

Parameters	Multi-layer perceptron	Radial basis function
Hidden layers	1	1
Input layers	1	1
Hidden neurons	5	5
Output neurons	1	1
Learning rate	0.2	0.051

5. Simulasyon results

To assess the effectiveness of the proposed controller, simulation studies are carried out for reactive power increase and line impedance variation conditions and overload conditions in two bus system and the reactive power increase in nine bus system.

5.1 Two bus simple system

To test the performance of the proposed SVC controller, the two bus power system shown in Fig.1 is introduced. Augmentation scenarios are considered as load

disturbance. The objective is to fix the voltage magnitude of the bus at 1 p.u. during simulation.

The steady state load demand is modeled through the parameter P_d , under the assumption that reactive power load demand is directly proportional to the active power demand, i.e., $Q_d = k.P_d$; this parameter is used here to carry out the voltage collapse studies. SVC operated capacitive mode provide out compensation effect for power system stability. To simplify the stability analysis, the resistance and line susceptance are neglected ($R=0, B_L=0$), $P_m=P_d$. The initial loading condition, as considered or not, as discussed below.

Table 2. The initial load conditions.

Generator inertia coefficient [M]	1 p.u
Generator damping coefficient [D_G]	1 p.u
Time constant [τ]	100 s
load power factor [k]	0.25
reactance of transmission line [X]	0.5
Active demand power [P_d]	0.6
Reactive demand power [$Q_d=k*P_d$]	0.25*0.6

5.1.1 Test 1 Increasing reactive power demand

The reactive power demand [Q_d] is chosen as the system parameter. In Test 1, the parameter Q_d is increased to test to simulate the dynamic voltage collapse phenomenon. In order to further demonstrate the effectiveness of the proposed controller, the level of reactive power demand is increased from $k=0.25$. to 0.5 in 3th seconds (Fig. 6.a). This progressive loading scenario will drive the power system from normal operating to voltage instability or collapse. Fig. 6 illustrates the response curves of the system against time of the sample system. In Fig.(6.b) shows the load bus voltage variation before and after the disturbance. It can be seen that the proposed both neural network controllers achieves good performance in voltage control of load bus (Fig. 6.b) It is tried to stabilize the load bus voltage at 1.0 pu by preventing the voltage collapse at the values. When demand reactive power (Q_d) are increased, neural controller prevents the voltage instability.

Voltage is below 0.7 pu without SVC. In Fig. 6c. Susceptance values are shown in both controller output and SVC output. RBFNN based controller catches the required susceptance value in a short time ($B_{SVC\text{controlled}}=0.392$ p.u) however, SVC model gives ($B_{SVC\text{dynamic model}}=0.388$ p.u) so RBFNN has shown the best performance. Figure 6d shows that generator angle increases without SVC state. As a result of this, the system goes towards to unstable state.

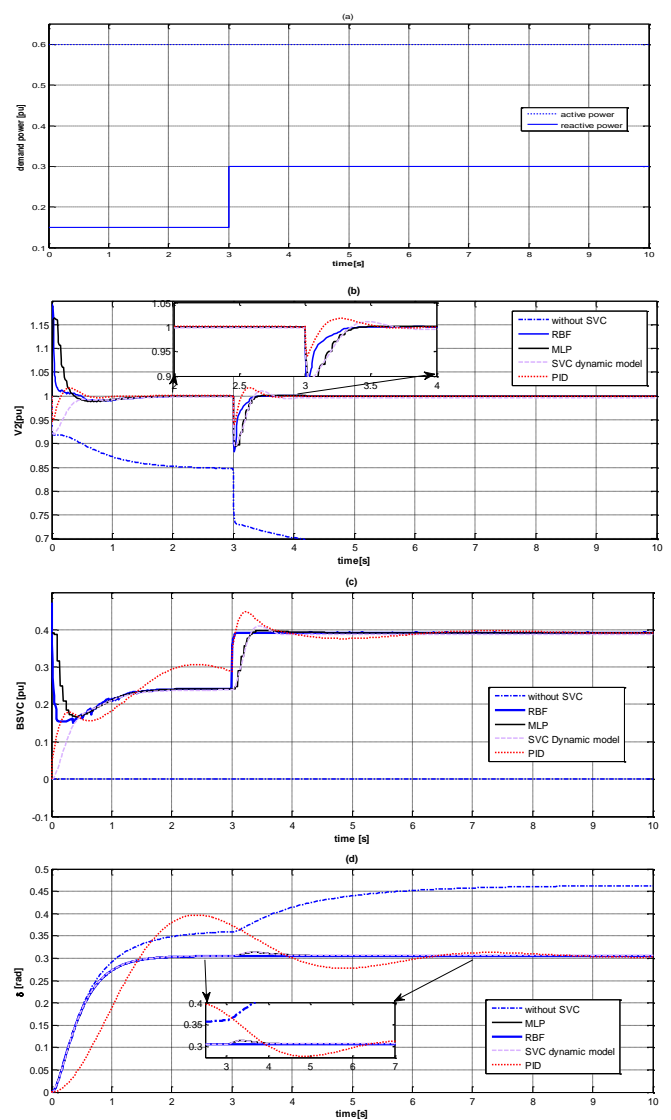


Fig. 6. The simple two bus system a) applied P_d Q_d b) variation of load bus voltage c) variation of the susceptance d) variation of the generator angle.

5.1.2. Test 2. Change in line impedance

It is assumed that at this part of training the reactance of the transmission line increased from 0.5 pu. to 1.0 pu by detaching one of the parallel lines as a results of error occurred at the transmission line (Fig. 7.a). The simulation results are shown in Fig. 7.

It can be seen that the proposed controllers achieves good performance in voltage control of load bus. In RBFNN- based control, load bus voltage reaches the rated value (1.0 p.u) quickly as compared MLP-based control (Fig 7.b).

After the first peak, RBFNN controller returns to the previous value smoothly. The voltage collapse existed after the disturbance effect in the system without SVC. From the above results, we see that voltage stability can be improved by the proposed controllers.

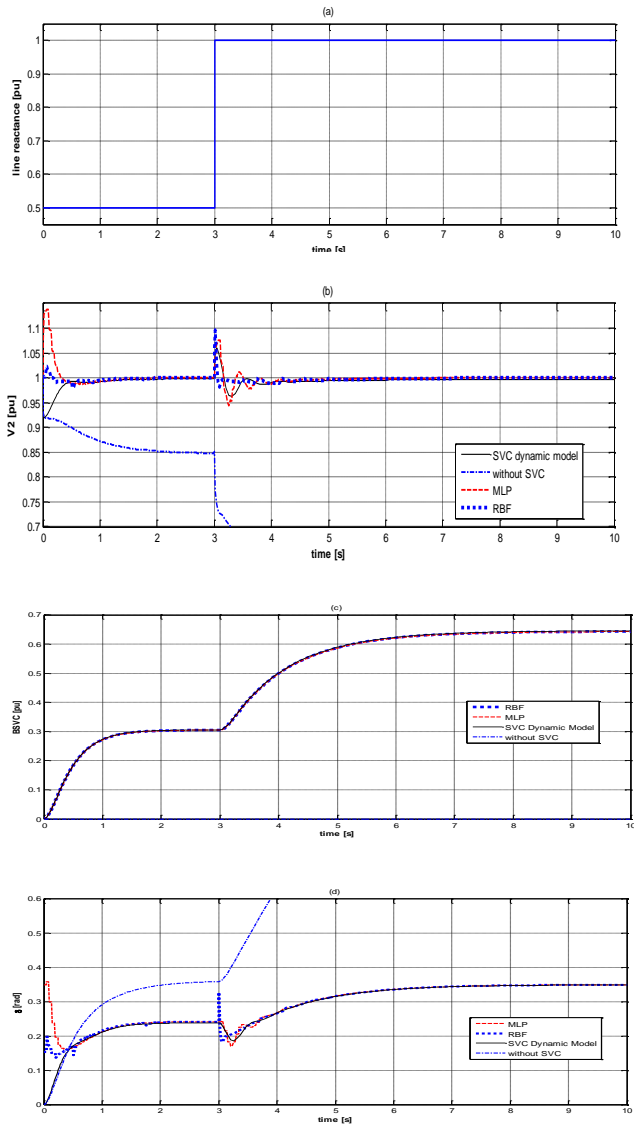


Fig. 7. Two bus system a) Applied line reactance changing b) variation of load bus voltage c) Variation of the susceptance d) variation of the generator angle.

In order to make comparison, output and error variations related to the proposed controllers are also investigated. Error curves are obtained according to the reference signal which is 1 per unit. At the end of the period of training, error signals in voltage signals are given at Fig. 8a-b. It is seen from these figures that smoothness is more in RBFNN-based controller than in MLPNN-based controller. It is seen from Figs. 8b and 8e multilayer perceptron network controller small oscillations occurred at 3th second, where the disturbance is applied. This controller caught the reference signal with a small delay.

But both the controllers managed to catch the reference signal successfully. This situation can be seen in Fig. 8b obviously. The Fig. 8e was drawn in order to observe the oscillations well.

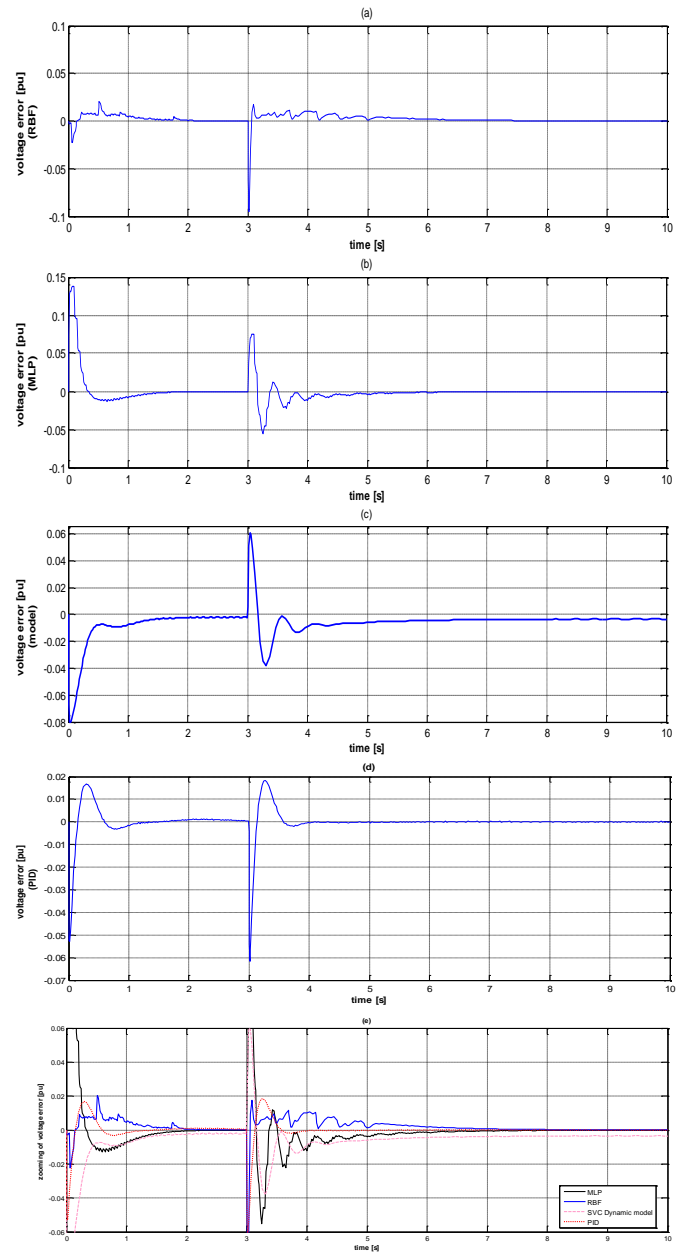


Fig. 8. Trained neural network and SVC dynamic model for a) error RBF network variations of load bus voltage b) error MLP network variations of load bus voltage c) error SVC dynamic model of load bus voltage d) error PID controller of load bus voltage e) zooming of network errors.

6. Applying to N-Bus power systems

The ANN -based SVC is implemented to in the three machine nine-bus system with three machine (WSCC system). The one line diagram of WSCC system is given Fig. 9. Details of the system data are given in Ref.[35]. Obtained conclusions result from load flow calculation shows in Table 3.

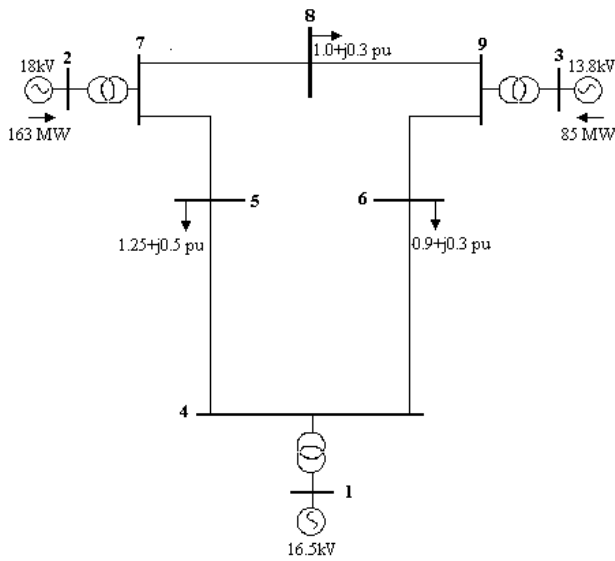


Fig. 9. Nine bus WSCC network.

Nine-bus power system which shown in Fig. 9 is reduced to two bus power system by using “The Reducing Bus Method”. Bus no 5 is chosen as critical bus due to the voltage value under 1.0 p.u. The power system is reduced to two bus system that consist of slack bus and bus no 5 whereas protecting the structure of nine bus system. Bus admittance matrix $Y_{bus_{red}}$ is achieved equation, as follows;

$$Y_{bus_{red}} = \begin{bmatrix} 0.6649 - j7.5136 & -0.5304 + j7.5640 \\ -0.5304 + j7.5640 & -0.1526 - j7.3574 \end{bmatrix}$$

where, the parameters of pi equivalent circuit having the 2-bus are $\dot{A} = 0.9665 - j.0879$, $\dot{B} = 0.0092 + j0.13160$, $\dot{C} = 0.5486 + j0.2436$, $\dot{D} = 0.9946 + j0.0182$

The stable operation point of reduced bus 5 is illustrated in Fig. 10. It is seen that voltage and angle values are the same with unreduced (original) system.

Table 3. Power flow results of nine bus system (without SVC).

Bus no	Bus type	V p.u.	δ (deg.)	P(MW)	Q(MVar)
1	Slack	1.0400	0.000	71.64	27.045
2	PV	1.025	9.280	163.00	6.653
3	PV	1.025	4.664	85.00	-10.859
4	PQ	1.0258	-2.216	0.00	0.000
5	PQ	0.9956	-3.988	-126.01	-50.440
6	PQ	1.0127	-3.687	-87.76	-29.250
7	PQ	1.0258	3.719	0.00	0.000
8	PQ	1.0159	0.727	-96.90	-33.910
9	PQ	1.0324	1.966	0.00	0.000

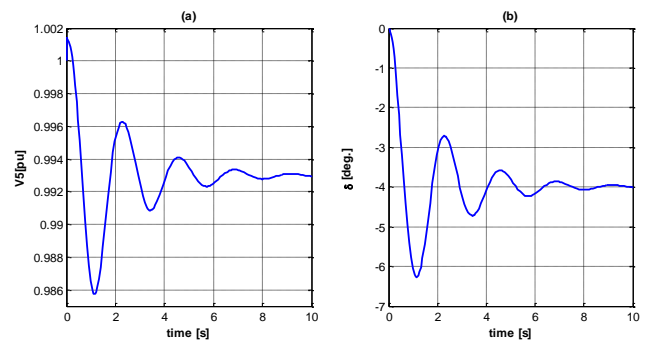


Fig. 10. In the bus 5 for loading condition of 1.25+ 0.5 p.u a) Load voltage b) Difference with load and generator angle oscillations ($\delta = \delta_1 - \delta_2$).

The performance and effectiveness of the proposed controller has been evaluated by simulating 9 bus test system. In order to keep voltage of bus 5 at 1 p.u one SVC is placed.

In Fig. 10a, the voltage of the system without SVC system is similar to the value obtained with the power flow. The proposed ANN controllers compared with conventional PID controller. With the initial power flow conditions, the level of reactive power demand is increased from 0.5 to 1.0 pu 5 s. The variation of bus voltage and susceptance of SVC are shown in Fig. 11a and Fig. 11b respectively to compare. The proposed ANN based controller has a less settling time than PID controller. It is clear that the best results are obtained by RBFNN controller is better than MLPNN and the PID controller.

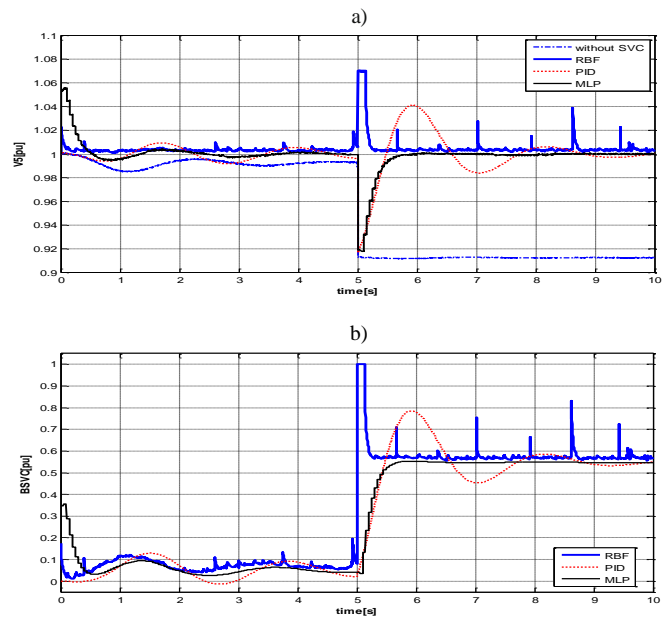


Fig. 11. Nine bus system a) variation of load bus 5 voltage b) Variation of the susceptance.

7. Conclusions

In this paper, two contributions are provided for is made to voltage stability enhancement. Firstly a novel bus reducing method, with the original system structure protected, is proposed. Secondly, a novel voltage stability enhancement method is proposed using on-line trained ANN based SVC controllers. The proposed controllers are trained by using, two types of learning methods: Multi layer perceptron and radial basis function. The simulation results shows that the proposed controllers provide a fast learning by finding the target susceptance value of SVC, and thus, improved voltage stability. The proposed controllers also tracked the reference signal successfully even though the applied disturbance effect.

When both controllers are compared to each other, RBFNN controller has much more performance due to reaching to stable state with smaller oscillations hence, smaller error rates.

Appendix A

The calculation of power flows is performed with all of the available information given in the form of interconnection of nodes and power injections. All of the system interconnections between nodes are combined into a single matrix known as the \mathbf{Y}_{bus} , or the admittance bus matrix, (Figure.12.a) [36]. Where, n is the number of buses; n_g , the number of generator and n_l , is the number of loads.

A.1 Two-port network implementation

According to voltage stability, except for load bus defined as critical values with a P-V bus chosen as slack bus, after it is obtained voltage and current profile of all power system using load flow in order to any load. Our proposed method is that power injections of all other buses, with scrutinized current directions, are added to bus admittance matrix. Thus the system is protected in order to that loading condition. Except for concerning bus and slack bus, all other buses are reduced by applied "Bus Reducing Technique" to newly attained "Bus Admittance Matrix" as shown Fig. 12.

Note that the two port models, which implies that; their admittance matrix is symmetric, i.e. $Y_{ij} = Y_{ji}$ and they can be represented by a pi-equivalent as shown in Fig. 12c

$$Y_{bus_{red}} = \begin{bmatrix} Y_{ii} & Y_{ij} \\ Y_{ji} & Y_{jj} \end{bmatrix} = \begin{bmatrix} y_{ij} + y_{i0} & -y_{ij} \\ -y_{ji} & y_{ji} + y_{j0} \end{bmatrix} \quad (18)$$

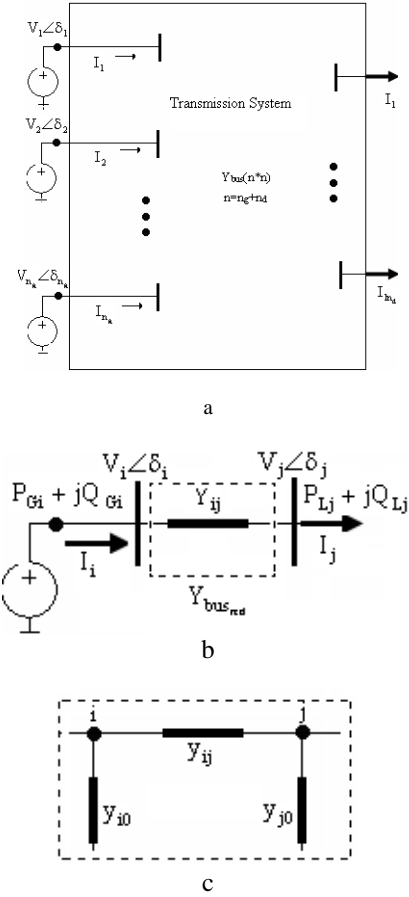


Fig. 12. (a). Current flow conventions, (b) Reduced system (c) Pi-equivalent of reciprocal two-ports.

To illustrate the power flow equations, the power flow across the general two-port network element connecting buses i and j shown in Fig. 12.b is considered and the following equations are obtained. The injected active and reactive power at i.bus (P_{gi} and Q_{gi})

$$P_{gi} = V_i V_j (c_1 \cos \delta + c_2 \sin \delta) + \frac{V_i^2 (d_1 b_1 + d_2 b_2)}{b_1^2 + b_2^2} - \dots - \frac{V_i V_j}{b_1^2 + b_2^2} [(d_1 b_1 + d_2 b_2)(a_1 \cos \delta + a_2 \sin \delta) + \dots + (d_1 b_2 - d_2 b_1)(a_2 \cos \delta - a_1 \sin \delta)] \quad (19)$$

$$Q_{gi} = V_i V_j (c_1 \sin \delta - c_2 \cos \delta) + \frac{V_i^2 (d_1 b_2 - d_2 b_1)}{b_1^2 + b_2^2} - \dots - \frac{V_i V_j}{b_1^2 + b_2^2} [(d_1 b_2 - d_2 b_1)(a_1 \cos \delta + a_2 \sin \delta) - \dots - (d_1 b_1 + d_2 b_2)(a_2 \cos \delta - a_1 \sin \delta)] \quad (20)$$

similarly,

$$P_{ij} = \frac{V_i V_j (b_1 \cos \delta + b_2 \sin \delta) - V_j^2 (a_1 b_1 + a_2 b_2)}{b_1^2 + b_2^2} \quad (21)$$

$$Q_{ij} = \frac{V_i V_j (b_2 \cos \delta - b_1 \sin \delta) - V_j^2 (a_1 b_2 - a_2 b_1)}{b_1^2 + b_2^2} \quad (22)$$

In order to SVC connected to j . Bus, reactive power $V_j^2 B_{\text{svc}}$ produced by SVC is added as additional Q_{ij} reactive power. Where pi equivalent network constants of two-ports reduced system are $\dot{A} = a_{1+j}a_2$, $\dot{B} = b_{1+j}b_2$, $\dot{C} = c_{1+j}c_2$, $\dot{D} = d_{1+j}d_2$

References

- [1] C. Schauder, M. Gernhardt, E. Stacey, T. W. Cease, A. Edris, *IEEE Trans. Power Del.*, **10**(7), 1486 (1995).
- [2] B. H. Chang, Y. B. Yoon, *Proc. KIEE*, **47**, 5–12 (1998).
- [3] Baiyat Samir A. Al, *The Arabian Journal for science and Engineering*, **30**(1B), (2005).
- [4] Chamni Jaipradidthan, J. Wang, X. Liao, Z. Yi(Eds) ISSN 668 (2005).
- [5] Vinod Kumar, R. R. Joshi, *Proc. of national conference on emerging Computational Technique and their application*, ECTTA, Jodhpur, India, 87 (2005).
- [6] D. Thukaram, Abraham Lomi, *Electric power system Research*, **54**(2), 139 (2000).
- [7] M. J. Laufenberg, M. A. Pai, K. R. Padiyar, *Electric Power and Energy Systems*, (19), 339 (1997).
- [8] P. Kundur, New York. Mc Graw-Hill, Inc, 1993.
- [9] J. R. Smith, D. A. Pierre, I. Sadighi, M. H. Nehrir, J. F. Hauer, *IEEE Transaction on Power Systems*, **4**(3), 1017 (1989).
- [10] D. Harikrishna, N. V. Srikanth, *India Conference (INDICON) Annual IEEE*, 1-4 (2009).
- [11] M. Sridhar, K. Vaisakh, K. Murthy, *Emerging Trends in Engineering and Technology (ICETET) 2nd International Conference on*, 985-990 (2009).
- [12] J. Wang, C. Fu, Y. Zhang, *IEEE Transactions on Industrial Electronics*, **55**(4), 1658 (2008).
- [13] Lan-fang Li, Kai- Pei Liu, Li ma, *IEEE/PES2005 Transmission and distribution Conference & Exhibition: Asia and Pasific Dalian, China*.
- [14] J. Lu, M. H. Nehrir, D. A. Pierre, *Electric Power Systems Research* **68**, 113 (2004).
- [15] N. Karpagam, D. Devaraj, *International Journal of Electrical and Electronics Engineering*, **3**(10), 625 (2009).
- [16] A. Albakkar, O. P. Malik, *16TH National power System Conference*, 237-242 (2010).
- [17] Jiang Tie-zheng, C. Chen, Y. Cao Guo, *Electr. Electron. Eng. China* **4**, 380 (2006).
- [18] Y. Wang, H. Chen, R. Zhou, *Electrical Power and Energy Systems*, **22**, 463 (2000).
- [19] R. Yan, Z. Y. Cong, T. K. Saha, J. Ma, *Power and Energy Society General Meeting, Conversion and Delivery of Electrical Energy in the 21st Century*, 1-7 (2008).
- [20] İ. K. Said, M. Pirouti, *International Journal of Computer and Electrical Engineering*, **1**(1), (2009).
- [21] D. Niebur, T. S. Dillon(editors), *Crl Publishing Ltd, U.K.*1996.
- [22] K. Girish, I.A.R.I. New Delhi,110012.
- [23] D. J. Hill, I. M. Y. Mareels, *IEEE Trans Circuits and Systems*, **37**(11), 1416 (1990).
- [24] V. Ajarapu, B. Lee, *IEEE Trans. Power System.*, **17**(1), 24 (1992).
- [25] I. Dobson, H. D. Chiang, *Syst Control Lett.* **13**, 253 (1989).
- [26] *IEEE/PES Power system stability Subcommittee Special Publication*, product no. Sp 101 PSS, Final document, August 2002.
- [27] Wei Gu, F. Milano, P. Jiang, G. Tang., *Electric Power System research*, **77**, 234 (2007).
- [28] H. T. Nguyen, N. R Prasad, C. L. E. A Walker, *CRC press*, 2002.
- [29] H. Demuth, M. Beale, *Ver.4, the Mathworks*.
- [30] A. S. Yilmaz, Z. Özer, *Expert Systems with Applications*, **36**, 9767 (2009).
- [31] Zurada, M. Jacek., *West Publishing Company, USA*, 1992.
- [32] N. K. Kasabov, *A Bradford Book/The MIT Pres*, 1998.
- [33] M. A. Arbib, (Ed)., *A Bradford Book, The MIT Pres*, 2003.
- [34] M. Ö. Efe, *Yapay Sinir Ağları ve Uygulamaları.*, Boğaziçi Üniversitesi, İstanbul, 141s.
- [35] P. Anderson, A. Fouad, *Power System Control and Stability*, Ames, IA: Iowa State University Press, 1977.
- [36] N. P. Padhy, M. A. Moamen abdel, *Electric Power System research*, **74**, 341 (2005).

*Corresponding author: kabaci@mersin.edu.tr